Available online at www.sciencedirect.com
SCIENCE DIRECT®
Journal of Magnetic Resonance 173 (2005) 296–304
JMR Journal of Magnetic Resonance
www.elsevier.com/locate/jmr

MAS NMR with and without double-quantum filtration at and near the $n = 0$ rotational resonance condition

Matthias Bechmann[1], Angelika Sebald[*,1]

Bayerisches Geoinstitut, Universität Bayreuth, D-95440 Bayreuth, Germany

Received 26 September 2004; revised 20 December 2004
Available online 1 February 2005

Abstract

Spectral lineshapes of MAS NMR spectra of dipolar (re)coupled spin pairs exhibiting considerable chemical shielding anisotropies at and near the so-called $n = 0$ rotational resonance (R^2) condition are considered. The $n = 0$ R^2 condition is found to be not extremely sharp. Anisotropic interaction parameters such as chemical shielding tensor orientations and the magnitude of the dipolar coupling constant remain sensitively encoded in such lineshapes even when differences in isotropic chemical shielding values of up to 400 Hz (corresponding to ca. half the size of the dipolar coupling constant) are present. Additional double-quantum filtration (DQF) may enhance the sensitivity of spectral lineshapes to anisotropic interaction parameters for even larger differences in isotropic chemical shielding values. The dependence of the DQF efficiency on spin-system parameters as well as on external parameters (Larmor and MAS frequencies) is investigated. Away from R^2 conditions a trend to lower DQF efficiencies is found whereas some spin-system parameters are more sensitively encoded in the corresponding spectral lineshapes. Our study is based on numerical simulations, with the known parameters of the ^{31}P spin pair in $Na_4P_2O_7 \cdot 10H_2O$ representing our model case.

Keywords: MAS NMR; Rotational resonance; Double-quantum filtration; Numerical simulations

1. Introduction

Amongst the numerous solid-state NMR techniques designed to recouple anisotropic interactions in homo- and heteronuclear spin systems under magic angle spinning (MAS) conditions [1,2], the rotational resonance (R^2) phenomenon is quite unique [3–5]. R^2 recoupling is not achieved by the application of r.f. pulses but is triggered by the mechanical spinning of the rotor at specific MAS frequencies, matching small integer multiples of the isotropic chemical shielding difference ω_{iso}^{Δ} in homonuclear pairs of spins $S = 1/2$ such that $\omega_{iso}^{\Delta} \approx n\omega_r$, where n is a small integer. Numerous studies in the literature have been concerned with the theoretical description of the R^2 phenomenon [6–10], with the exploitation of straightforward R^2 MAS NMR spectra for purposes of complete characterisation of small isolated clusters of spins [11–14] as well as of extended spin systems [15,16], with combining R^2 and double-quantum filtration (DQF) [17–21], and with expanding the applicability of the R^2 phenomenon to spin systems featuring small homonuclear dipolar coupling constants [22,23].

Here we will focus on a specific R^2 condition, the so-called $n = 0$ R^2 condition [24]. This condition arises for homonuclear spin pairs with vanishing difference in isotropic chemical shielding, $\omega_{iso}^{\Delta} = 0$, but with differing orientations of the two chemical shielding tensors. As there is no difference in isotropic shielding, the $n = 0$ R^2 condition persists at arbitrary spinning frequencies, including spinning frequencies greatly exceeding the

* Corresponding author. Fax: +49 921 55 3769.
E-mail address: angelika.sebald@uni-bayreuth.de (A. Sebald).
[1] Present address: Universität Dortmund, Fachbereich Physik, D-44221 Dortmund, Germany.

1090-7807/$ - see front matter © 2005 Elsevier Inc. All rights reserved.
doi:10.1016/j.jmr.2004.12.012

value of the dipolar coupling constant within the spin pair. The effect is the consequence of an intrinsic property of a given spin pair and obviously, if present but unwanted, a $n = 0$ R^2 condition cannot be avoided or circumvented by choice of external experimental parameters such as MAS frequency or magnetic field strength. For instance, spins belonging to molecular sites related to each other by mirror symmetry or by a C_2 symmetry axis fulfill the requirements for the occurrence of the $n = 0$ R^2 condition [11,24,25]. In fact, the presence of such symmetry-related (molecular) sites is fairly common in small molecules as well as in extended three-dimensional network structures. Even more common as a structural motif are pairs of sites representing a situation close to the $n = 0$ R^2 condition, that is the two sites are not strictly related by a proper symmetry operation but are not deviating much from this situation. In terms of MAS NMR, this $n \approx 0$ R^2 scenario will often lead to spin pairs characterised by a small difference in isotropic chemical shielding $\omega^{\Delta}_{\mathrm{iso}}$, with $\omega^{\Delta}_{\mathrm{iso}}$ often being smaller than any of the remaining interaction parameters. Distinguishing MAS NMR spectra of spin pairs at or near the $n = 0$ R^2 condition from each other is not possible simply by inspection, the distinction requires careful analysis by means of numerically exact simulations [26].

Because of the common occurrence of structural features leading to MAS NMR conditions at or near the $n = 0$ R^2 condition, in the following we will investigate in some detail the dependence of $n = 0$ and $n \approx 0$ R^2 conditions on spin-system properties and on external experimental parameters. We will consider straightforward MAS NMR spectra as well as spectra obtained under DQF conditions. Our starting point is represented by the known properties of the ^{31}P spin pair in $Na_4P_2O_7 \cdot 10H_2O$ [11]: since the two phosphorus sites in the P_2O_7 unit are related by a C_2 axis bisecting the P–O–P bond angle, the two ^{31}P spins constitute a $n = 0$ R^2 case. Our investigation will mainly rest on numerically exact simulations.

2. Experimental

2.1. ^{31}P MAS NMR

Some experimental ^{31}P MAS NMR spectra of $Na_4P_2O_7 \cdot 10H_2O$ (commercially available (Aldrich Chemicals)) were recorded on Bruker MSL 200 and MSL 300 NMR spectrometers. The corresponding ^{31}P Larmor frequencies $\omega_0/2\pi$ are -81.0 and -121.5 MHz, respectively. ^{31}P chemical shielding is quoted with respect to $\omega^{CS}_{\mathrm{iso}} = 0$ ppm for the ^{31}P resonance of 85% H_3PO_4. MAS frequencies were generally in the range $\omega_r/2\pi = 2400$–8000 Hz and were actively controlled to within ± 2 Hz. The sample was contained in a standard 4 mm o.d. ZrO_2 rotor. Cross polarisation with a contact time of 1 ms was employed, ^{31}P $\pi/2$ pulse durations were 3.0 μs, c.w. ^{1}H decoupling with amplitudes of 83.3 kHz was applied during signal acquisition.

The R^2-DQF MAS NMR experiment chosen for recording some experimental spectra as well as for all simulations, is the simple COSY-like sequence $CP_{(x)}$–τ–$(\pi/2)_{(y)}$–Δ–$(\pi/2)_{(\phi)}$–acquisition [17] where ϕ indicates phase cycling suitable for DQF [27]. The duration of Δ was fixed as $\Delta = 3$ μs, the duration of τ was varied.

2.2. Definitions, notation, and numerical simulations

Shielding notation [28] is used throughout. For the interactions $\lambda = CS$ (chemical shielding), $\lambda = D$ (direct dipolar coupling), and $\lambda = J$ (indirect dipolar (J) coupling) the isotropic part $\omega^{\lambda}_{\mathrm{iso}}$, the anisotropy $\omega^{\lambda}_{\mathrm{aniso}}$, and the asymmetry parameter η^{λ} relate to the principal elements of the interaction tensor ω^{λ} as follows [29]: $\omega^{\lambda}_{\mathrm{iso}} = (\omega^{\lambda}_{xx} + \omega^{\lambda}_{yy} + \omega^{\lambda}_{zz})/3$, $\omega^{\lambda}_{\mathrm{aniso}} = \omega^{\lambda}_{zz} - \omega^{\lambda}_{\mathrm{iso}}$, and $\eta^{\lambda} = (\omega^{\lambda}_{yy} - \omega^{\lambda}_{xx})/\omega^{\lambda}_{\mathrm{aniso}}$ with $|\omega^{\lambda}_{zz} - \omega^{\lambda}_{\mathrm{iso}}| \geqslant |\omega^{\lambda}_{xx} - \omega^{\lambda}_{\mathrm{iso}}| \geqslant |\omega^{\lambda}_{yy} - \omega^{\lambda}_{\mathrm{iso}}|$. For indirect dipolar coupling $\omega^{J}_{\mathrm{iso}} = \pi J_{\mathrm{iso}}$, and for direct dipolar coupling $\eta^{D} = \omega^{D}_{\mathrm{iso}} = 0$ and $\omega^{D_{ij}}_{\mathrm{aniso}} = b_{ij} = -\mu_0 \gamma_i \gamma_j \hbar/(4\pi r^3_{ij})$, where γ_i, γ_j denote gyromagnetic ratios and r_{ij} is the internuclear distance between spins S_i, S_j. The Euler angles $\Omega_{IJ} = \{\alpha_{IJ}, \beta_{IJ}, \gamma_{IJ}\}$ [30] relate axis system I to axis system J, where I, J denote P (principal axis system, PAS) and C (crystal axis system, CAS), respectively. Here it is convenient to define the PAS of the dipolar coupling tensor ω^{D}_{ij} as the CAS, $\Omega^{D_{ij}}_{PC} = \{0, 0, 0\}$.

Our procedures for numerically exact spectral lineshape simulations and iterative fitting are fully described and discussed in detail elsewhere, in particular addressing the $n = 0$ R^2 condition for isolated homonuclear spin pairs [11] and various $n = 0,1,2$ R^2 conditions in an isolated homonuclear ^{13}C four-spin system [13]. In general, these numerical procedures employ the REPULSION [31] scheme for the calculation of powder averages, implement some of the routines of the GAMMA package [32] and use, where possible, the γ-COMPUTE approach [33–36]. The pulse sequence of the R^2-DQF experiment [17] is not synchronous with the MAS rotation period and simulation of the underlying spin dynamics hence requires application of the so-called direct method for the calculation of the time evolution. Calculations may be considerably accelerated by using a cluster of processors and splitting up, for instance, the calculation of powder averages into several parallel calculations. The Linux PC cluster used here consists of 16 processors (450 MHz). This combination of hard- and software leads to typical computation times of 23 s for the calculation of a R^2-DQF MAS NMR spectrum. Calculations of error scans and other error minimisation tasks employ the MINUIT [37] and MATLAB packages [38].

Table 1 lists the parameters of the ^{31}P spin pair in $Na_4P_2O_7 \cdot 10H_2O$ [11].

Table 1
NMR parameters of the ^{31}P spin pair in $Na_4P_2O_7\cdot 10H_2O$ [11]

	^{31}P1	^{31}P2
ω_{iso}^{CS} (ppm)[a]	+2.3	+2.3
ω_{aniso}^{CS} (ppm)	-79 ± 1	-79 ± 1
η^{CS}	0.35 ± 0.1	0.35 ± 0.1
α_{PC}^{CS} (°)[a]	-117 ± 4	-117 ± 4
β_{PC}^{CS} (°)[a]	-23 ± 2	157 ± 2
γ_{PC}^{CS} (°)[a]	0 ± 6	180 ± 6
$b_{12}/2\pi$ (Hz)	−791	−791
$^2J_{iso}$ (Hz)	-19.5 ± 2.5	-19.5 ± 2.5

[a] The two ^{31}P chemical shielding tensors are related by C_2 symmetry; the Euler angles are given relative to the principal axis system of the ^{31}P1–^{31}P2 dipolar coupling tensor.

3. Results and discussion

Some experimental and best-fit simulated (see Table 1) $n = 0$ R^2 ^{31}P MAS NMR spectra of $Na_4P_2O_7\cdot 10H_2O$, with and without DQF, are shown in Fig. 1, illustrating the typical lineshape effects, broadenings and splittings, encountered at the $n = 0$ R^2 condition as well as the commonly observed dispersion lineshapes under these DQF conditions. The ^{31}P spin pair in $Na_4P_2O_7\cdot 10H_2O$ may be considered as a prototype of an isolated spin pair where chemical shielding is the largest anisotropic interaction tensor but not overwhelmingly so: with the ^{31}P chemical shielding anisotropy amounting to $\omega_{aniso}^{CS} = -79 \pm 1$ ppm, at $\omega_0/2\pi = -81.0$ MHz and at $\omega_0/2\pi = -121.5$ MHz, ω_{aniso}^{CS} is about 8–10 times larger

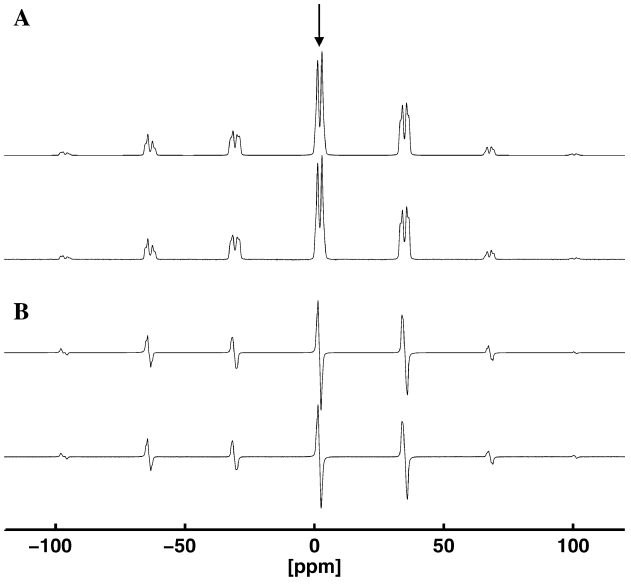

Fig. 1. ^{31}P MAS NMR spectra of $Na_4P_2O_7\cdot 10H_2O$ ($\omega_0/2\pi = -121.5$ MHz, $\omega_r/2\pi = 4000$ Hz). (A) Conventional $n = 0$ R^2 MAS NMR spectrum, experimental spectrum (bottom trace) and best-fit simulation (top trace). (B) $n = 0$ R^2-DQF MAS NMR spectrum, experimental spectrum (bottom trace) and best-fit simulation (top trace). The arrow indicates isotropic chemical shielding, parameters see Table 1.

than the dipolar coupling constant ($b_{ij}/2\pi = -791$ Hz), whereas the indirect coupling constant, $^2J_{iso}(^{31}P,^{31}P) = -19.5 \pm 2.5$ Hz is comparatively small [11]. This constellation is not only typical for ^{31}P spin systems in many inorganic condensed phosphates but may also be encountered, at various magnetic field strengths, in spin systems composed of other isotopes in a wide range of chemical compounds, including ^{13}C in isotopically labelled organic molecules. Accordingly, our results do not only reflect the NMR properties of a particular spin system in a particular compound but should be seen as representative for spin systems with properties similar to those of the ^{31}P spin pair chosen as our example.

In the following we will first consider lineshapes of a range of MAS NMR spectra at and near the $n = 0$ R^2 condition, focussing on the sensitivity with which various anisotropic interaction tensors are reflected by these spectral lineshapes, both with and without the application of DQF. Section 2 will deal with aspects of DQF efficiencies, again for a range of differences in isotropic chemical shielding, covering the whole range from $\omega_{iso}^{\Delta} = 0$ up to values of ω_{iso}^{Δ} being equivalent to $n = 1$ R^2 conditions, assuming different Larmor and MAS frequencies.

3.1. Sensitivities of lineshapes to spin-pair parameters

All anisotropic interaction parameters present are usually sensitively encoded in the spectral lineshapes at the $n = 0$ R^2 condition (see Fig. 1, Table 1) at modest MAS frequencies. In practical terms this means that such experimental lineshapes may be used to extract these parameters by lineshape simulations in conjunction with iterative fitting approaches, and thus to characterise the parameters of a spin pair in a comprehensive way from few, experimentally straightforward spectra. Here we take essentially the opposite approach. We take the known set of parameters describing the ^{31}P spin pair in $Na_4P_2O_7\cdot 10H_2O$ and use these parameters to calculate hypothetical spectra for a range of values ω_{iso}^{Δ}, ranging from $\omega_{iso}^{\Delta} = 0$ to ω_{iso}^{Δ} being equivalent to the $n = 1$ R^2 condition. These calculations are carried out for several different Larmor frequencies $\omega_0/2\pi$ and for several different MAS frequencies $\omega_r/2\pi$. Each of these calculated spectra in a next step is subjected to computing error scans for each of the anisotropic interaction parameters of the spin pair. In this way a map is created that permits us to predict which parameters are likely to be sensitively encoded in MAS NMR spectra, depending on the value of the difference in isotropic chemical shielding, ω_{iso}^{Δ}, of the two spins in a spin pair.

The results of these calculations for the Euler angle β_{PC}^{CS} and for the dipolar coupling constant $b_{ij}/2\pi$ are summarised in Fig. 2, assuming straightforward MAS NMR spectra being recorded. The rows (A), (B), and (C) in Fig. 2 assume different MAS frequencies $\omega_r/2\pi =$

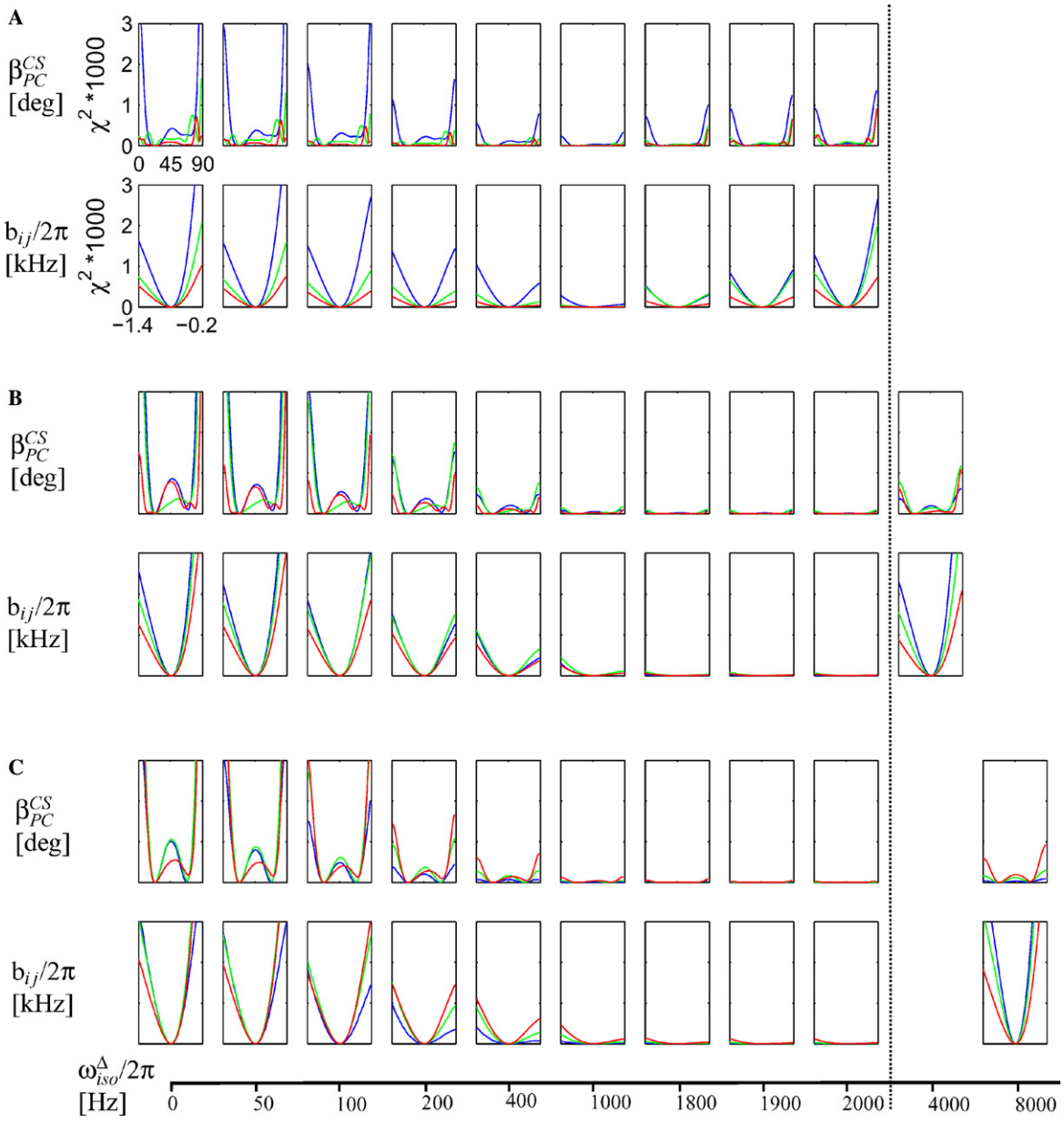

Fig. 2. Selection of error scans for β_{PC}^{CS} (0°–90°) and $b_{ij}/2\pi$ (−1400 to −200 Hz) each, based on simulated MAS NMR spectra (parameters see Table 1). In the columns from left to right ω_{iso}^{Δ} is incremented as indicated by the scale at the bottom. Colours indicate different Larmor frequencies where red corresponds to $\omega_0/2\pi = -202.5$ MHz, green to $\omega_0/2\pi = -121.5$ MHz, and blue to $\omega_0/2\pi = -81.0$ MHz, respectively. Scans are shown for $\omega_r/2\pi = 2000$ Hz (A), $\omega_r/2\pi = 4000$ Hz (B), and $\omega_r/2\pi = 8000$ Hz (C).

2 kHz, $\omega_r/2\pi = 4$ kHz, and $\omega_r/2\pi = 8$ kHz, respectively. The columns in Fig. 2 increment the value of ω_{iso}^{Δ} from $\omega_{iso}^{\Delta} = 0$ to ω_{iso}^{Δ} being equivalent to the three $n = 1$ R^2 conditions, as indicated by the scale at the bottom. The colours in each segment indicate three different Larmor frequencies, blue traces assume $\omega_0/2\pi = -81.0$ MHz, green traces $\omega_0/2\pi = -121.5$ MHz, and red traces $\omega_0/2\pi = -202.5$ MHz. Only the minimum regions of each error scan are plotted. The main findings are as follows. Clearly, the $n = 0$ R^2 condition is not extremely sharp. Independent of the Larmor frequency, always up to $\omega_{iso}^{\Delta} \approx 400$ Hz, that is up to $\omega_{iso}^{\Delta} \approx 0.5\ b_{ij}/2\pi$, both β_{PC}^{CS} and b_{ij} remain encoded in the spectral lineshapes. Increasing ω_{iso}^{Δ} further, covering the region inbetween the $n = 0$ R^2 condition and the $n = 1$ R^2 conditions, not surprisingly leaves a region in which none of these parameters are encoded in the lineshapes. In this intermediate region, spectra are strongly dominated by the magnitude of the chemical shielding tensors. Sensitivity of the spectral lineshapes to further anisotropic interaction parameters is recovered upon increasing ω_{iso}^{Δ} further, approaching the $n = 1$ R^2 regime. Again, also the $n = 1$ R^2 condition is not extremely sharp, displaying a similar $n \approx 1$ R^2 region as does the

$n = 0$ R^2 condition, spanning approximately ±400 Hz, equivalent to approximately 0.5 $b_{ij}/2\pi$.

Fig. 2 further indicates that, at and near the $n = 0$ R^2 condition, both the dipolar coupling constant b_{ij} and the Euler angle β_{PC}^{CS} are best defined from the lineshapes of ^{31}P MAS NMR spectra obtained at $\omega_0/2\pi = -81.0$ MHz. As far as b_{ij} is concerned one may be intuitively inclined to predict that this parameter might be best obtained from experimental spectra run at a moderate Larmor frequency. Regarding the orientation of the ^{31}P chemical shielding tensor, this finding may seem more surprising as one may tend to predict that chemical shielding tensor parameters may become more sensitively encoded as one operates at higher Larmor frequencies. An optimum Larmor frequency where simultaneously chemical shielding and dipolar coupling parameters are encoded with the highest sensitivities in spectral lineshapes of homonuclear spin pairs at or near the $n = 0$ R^2 condition depends on the ratio of the chemical shielding anisotropy $\omega_{\text{aniso}}^{CS}$ to the dipolar coupling constant b_{ij}, as well as on the spinning frequency ω_r. The optimum choice of experimental conditions is then in a regime where $\omega_{\text{aniso}}^{CS} \leqslant 8b_{ij}$ and $\omega_r \leqslant \omega_{\text{aniso}}^{CS} \leqslant 2\omega_r$. The same choice of the experimental parameters ω_r and ω_0 remains the optimum regime with the highest sensitivities of spectral lineshapes to all interaction parameters for a wide range of chemical shielding tensor orientations (simulations not shown). Fig. 2 illustrates another general trend. One can generally expect to be able to extract magnitudes of interaction tensors with the highest accuracy from those experimental spectra in which these parameters are encoded with the highest sensitivity. The situation regarding expected accuracies is slightly more complicated regarding the orientational parameters where highest sensitivities do not necessarily correlate with highest accuracies. For example (see Fig. 2A), β_{PC}^{CS} is most sensitively encoded at a Larmor frequency $\omega_0/2\pi = -81.0$ MHz, though with a fairly broad minimum-error region, whereas a slightly lower sensitivity combined with a more sharply defined minimum region is found at $\omega_0/2\pi = -121.5$ MHz.

Similar to the $n \approx 0$ R^2 scenario considered here, optimum experimental conditions exist for isolated spin-1/2 cases when aiming at the determination of the eigenvalues of the chemical shielding tensor from MAS NMR spectra, where an optimum choice of Larmor and MAS frequency would generate about 6–10 spinning sidebands [39]. Also for the full characterisation of some heteronuclear spin pairs from MAS NMR spectra an optimum choice of the experimental parameters can be predicted, where a ratio of ω_r:$b_{ij} \approx 1$:6 turns out the most suitable condition for full spectral analysis [40].

Next, we consider the spectral lineshapes resulting from additional application of DQF. This is summarised in Fig. 3. The set of error scans is identical to the set displayed in Fig. 2, except that now all error scans refer to spectral lineshapes obtained after application of a COSY-like DQF pulse sequence. Whereas under conventional MAS NMR conditions an intermediate regime of ω_{iso}^{A} exists where spectral lineshapes are insensitive to chemical shielding tensor orientations and dipolar coupling, no such regime exists anymore after DQF. Essentially for the entire range of values ω_{iso}^{A}, from the $n = 0$ R^2 condition all the way to the $n = 1$ R^2 condition, spectral lineshapes now reflect all anisotropic parameters of the spin pair. Note that in some regions orientational and dipolar coupling parameters are more sensitively encoded away from the $n = 0$ R^2 condition than at or very near the $n = 0$ R^2 condition. All other trends remain the same as under conventional MAS NMR conditions. This increased sensitivity of the lineshapes to all spin-system parameters could be seen as good news if one is aiming at the full characterisation of these parameters from spectral lineshapes. In fact, applying DQF even if not necessary for reasons of background suppression of unwanted signals, can be beneficial for the characterisation of homonuclear spin pairs at or near the $n = 0$ R^2 condition [26]. The vanishing of an intermediate regime inbetween R^2 conditions which is insensitive to orientational parameters, however, may also be an unwanted feature. For instance, when aiming to determine internuclear distances without having to pay attention to magnitudes and orientations of the chemical shielding tensors involved, sensitivity of experimental spectra to these parameters is certainly not a helpful feature. The extent and precise location of regions where spectra are highly sensitive to all spin-system parameters will vary slightly, depending on the pulse sequence used (including so-called γ-encoded pulse sequences [41]). Nevertheless, it is to be expected that almost always for certain regions over the range of ω_{iso}^{A} all spin-system parameters need to be taken into account to obtain precise information, for instance, about internuclear distances based on the evaluation of dipolar coupling interactions [42].

3.2. DQF efficiencies at and near the $n = 0$ R^2 condition

Excellent signal-to noise ratio in experimental spectra is an important prerequisite for the meaningful analysis of spectral lineshapes. Accordingly, consideration of DQF efficiencies plays an important part in the experimental work. Fig. 4 gives an overview of trends for the COSY-like DQF approach. Fig. 4A depicts DQF efficiencies at the $n = 0$ R^2 condition, plotted as a function of the duration of the excitation period τ, and considers the effect of different MAS frequencies ω_r. As one can see (from left to right), increasing ω_r leads to a decrease in overall DQF efficiency, and the overall maximum shifts to longer durations of τ. As usual, maxima of DQF efficiency occur when τ equals an integer

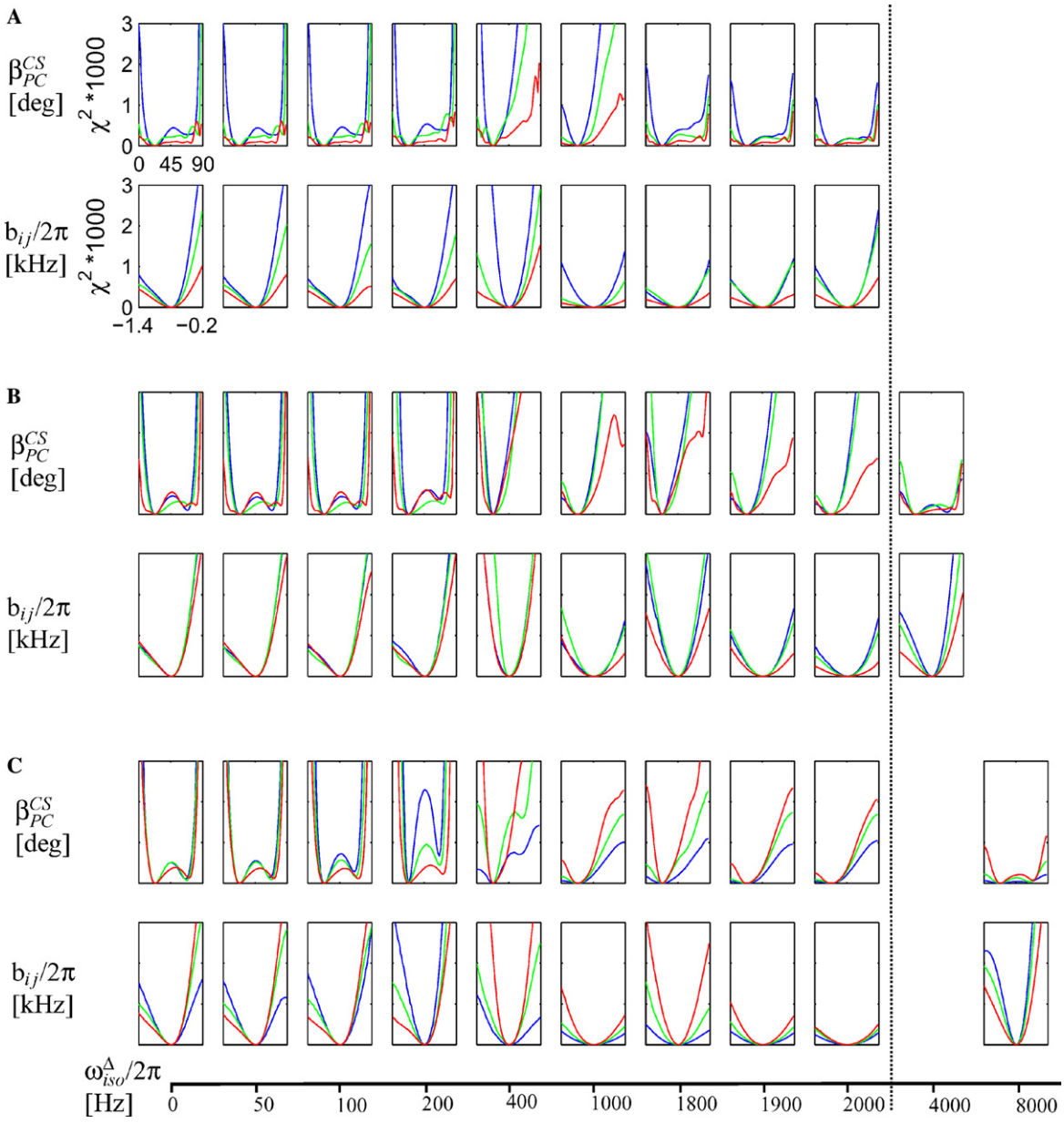

Fig. 3. Same as Fig. 2, except that now error scans are shown for R^2-DQF MAS NMR spectra with $\tau = 2$ ms.

multiple of a rotation period. Fig. 4B illustrates another practically important point. The only difference between this graph and Fig. 4A is that now ω_{iso}^{A} is taken as $\omega_{iso}^{A} = 400$ Hz, whereas before $\omega_{iso}^{A} = 0$. Obviously, away from the $n = 0$ R^2 condition, there is a general decrease in DQF efficiency with maxima in DQF efficiency now appearing at durations of τ that are quite different from those where maximum DQF efficiency occurs when the $n = 0$ R^2 condition is fulfilled. Fig. 4C expands on this aspect by depicting DQF efficiencies for several different durations of τ plotted as a function of ω_{iso}^{A}. The 'broadness' of the regions around the R^2 conditions with reasonable DQF efficiencies varies as a function of τ, as does the maximum DQF efficiency. DQF efficiencies of approximately 25% at the $n = 0$ R^2 condition and approximately 10% when $\omega_{iso}^{A} = 400$ Hz may seem rather low and will only be sufficient for some practical applications where signal-to-noise is not a limiting factor. In the presence of fairly large chemical shielding anisotropies, however, DQF efficiencies are generally low [41]. Amongst the many pulse sequences suitable for DQF under MAS conditions, the simple COSY-like sequence performs relatively well in the presence of large chemical shielding anisotropies [20].

Here we have not varied any of the spin-system parameters except ω_{iso}^{A}. Of course, also the relative magnitudes and orientations of ω_{aniso}^{CS} and b_{ij} generally play an important role in defining the maximum DQF effi-

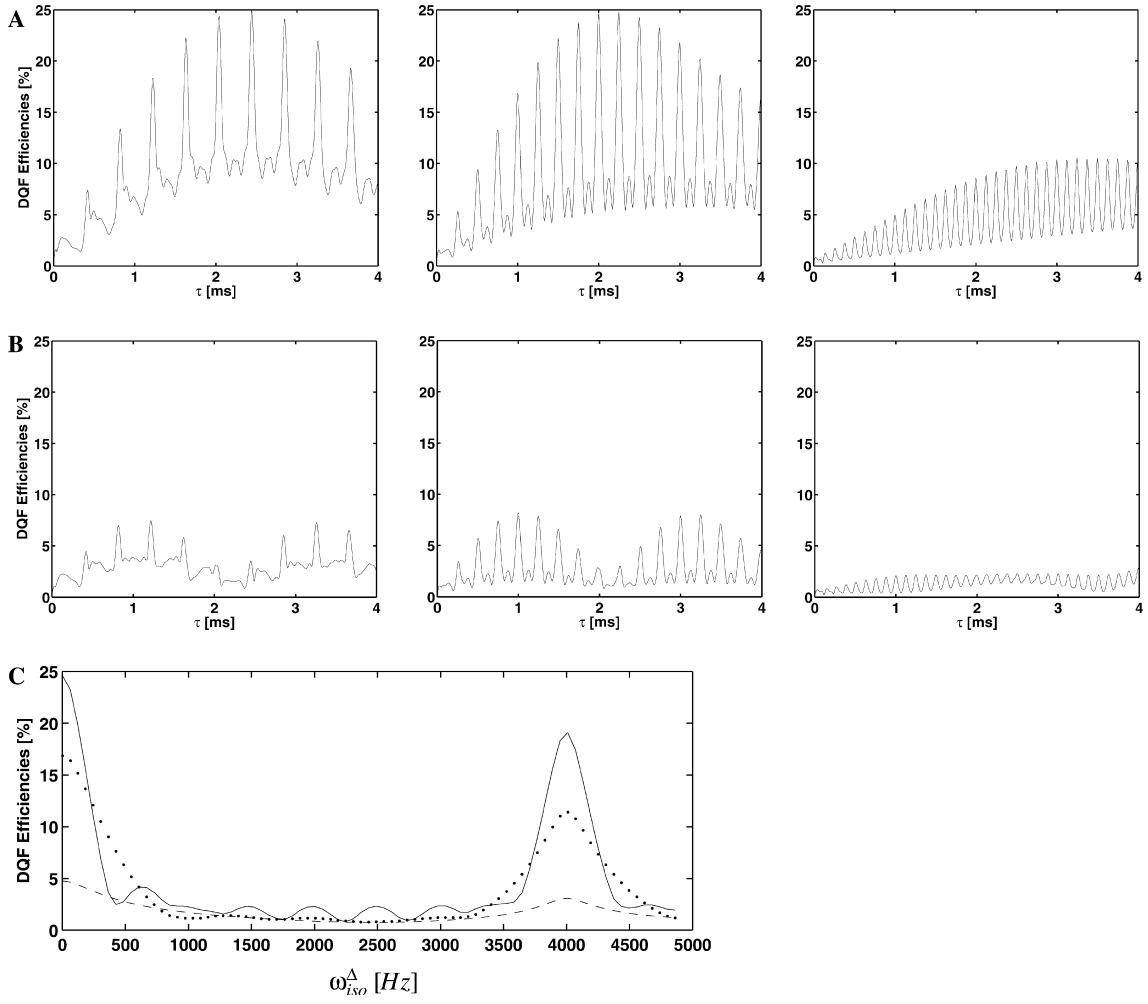

Fig. 4. DQF efficiencies plotted as a function of τ (A and B) and $\omega^{\Delta}_{\mathrm{iso}}$ (C); simulations based on spin-pair parameters given in Table 1 and assuming $\omega_0/2\pi = -121.5$ MHz. (A) $\omega^{\Delta}_{\mathrm{iso}} = 0$; from left to right $\omega_r/2\pi = 2454$ Hz, $\omega_r/2\pi = 4000$ Hz, and $\omega_r/2\pi = 8000$ Hz. (B) $\omega^{\Delta}_{\mathrm{iso}} = 400$ Hz; from left to right $\omega_r/2\pi = 2454$ Hz, $\omega_r/2\pi = 4000$ Hz, and $\omega_r/2\pi = 8000$ Hz. (C) $\omega_r/2\pi = 4000$ Hz, $\tau = 8\tau_r = 2$ ms (——), $\tau = 4\tau_r = 1$ ms (●●●), $\tau = \tau_r = 0.5$ ms (- - -).

ciencies. For instance, we find that increasing $\omega^{CS}_{\mathrm{aniso}}$ at the $n = 0$ R^2 condition tends to shift the DQF maximum to occur at longer durations of τ, whereas no such clear-cut trends can be seen away from the $n = 0$ R^2 condition.

4. Summary and conclusions

The so-called $n = 0$ R^2 condition covers a considerable range of values $\omega^{\Delta}_{\mathrm{iso}}$, from $\omega^{\Delta}_{\mathrm{iso}} = 0$ up to $\omega^{\Delta}_{\mathrm{iso}} \approx 0.5 b_{ij}$ (here ca. 400 Hz). This perseverance of linebroadening and -splitting effects may add complexity to the interpretation of simple MAS NMR spectra of dipolar coupled spin systems, for instance ^{31}P MAS NMR spectra of condensed phosphates or ^{13}C MAS NMR spectra of ^{13}C enriched compounds. On the other hand, this property lends a higher information content to simple MAS NMR spectra as these then sensitively reflect anisotropic spin-system parameters such as the orientation of chemical shielding tensors as well as dipolar coupling constant. Additional r.f. irradiation at and near the $n = 0$ R^2 condition by applying pulse sequences, for instance for purposes of DQF, may extend the occurrence of R^2 effects to even larger values $\omega^{\Delta}_{\mathrm{iso}}$. This may sometimes be a welcome feature. In many application circumstances aiming at the determination of internuclear distances, dependence of experimental data on magnitudes and orientations of chemical shielding tensors adds further complications. These effects are not easy to predict when dealing with spin systems characterised by largely unknown parameters but will mainly affect pairs of spins with similar isotropic chemical shielding values, displaying considerable chemical shielding anisotropies and relatively large dipolar coupling constants. Such R^2 effects may contribute systematically to e.g., the intensity of off-diagonal peaks in two-dimensional dipolar recoupling experiments. Since the evaluation of short-range dipolar coupling constants from such experiments usually is the starting point in series of experiments aiming to construct three-dimen-

sional structural constraints for multi-spin systems, we feel that it is important not to neglect these effects in the data analysis [42].

Acknowledgments

Financial support of our work by the Deutsche Forschungsgemeinschaft and by Aventis Pharma, Paris, is gratefully acknowledged. We thank X. Helluy, Würzburg, for his cooperation in the early stages of the project, and an unknown reviewer for constructive comments.

References

[1] A.E. Bennett, R.G. Griffin, S. Vega, Recoupling of homo- and heteronuclear dipolar interactions in rotating solids, in: B. Blümich (Ed.), Solid-State NMR IV: Methods and Applications of Solid-State NMR, NMR Basic Principles and Progress, vol. 33, Springer, Berlin, 1994, pp. 1–78.

[2] S. Dusold, A. Sebald, Dipolar recoupling under magic-angle-spinning conditions, in: G. Webb (Ed.), Annual Reports on NMR Spectroscopy, vol. 41, Academic Press, London, 2000, pp. 185–264.

[3] E.R. Andrew, A. Bradbury, R.G. Eades, V.T. Wynn, Nuclear cross relaxation induced by specimen rotation, Phys. Lett. 4 (1963) 99–100.

[4] D.P. Raleigh, M.H. Levitt, R.G. Griffin, Rotational resonance in solid state NMR, Chem. Phys. Lett. 146 (1988) 71–76.

[5] D.P. Raleigh, F. Creuzet, S.K. Gupta, M.H. Levitt, R.G. Griffin, Measurement of internuclear distances in polycrystalline solids: rotationally enhanced transfer of nuclear spin magnetization, J. Am. Chem. Soc. 111 (1989) 4502–4503.

[6] M.H. Levitt, D.P. Raleigh, F. Creuzet, R.G. Griffin, Theory and simulations of homonuclear spin pairs in rotating solids, J. Chem. Phys. 92 (1990) 6347–6364.

[7] A. Kubo, C.A. McDowell, One- and two-dimensional ^{31}P cross-polarization magic-angle-spinning nuclear magnetic resonance studies on two-spin systems with homonuclear dipolar and J coupling, J. Chem. Phys. 92 (1990) 7156–7170.

[8] A. Schmidt, S. Vega, The Floquet theory of nuclear magnetic resonance spectroscopy of single spins and dipolar coupled spin pairs in rotating solids, J. Chem. Phys. 96 (1992) 2655–2680.

[9] T. Nakai, C.A McDowell, An analysis of NMR spinning sidebands of homonuclear two-spin systems using Floquet theory, Mol. Phys. 77 (1992) 569–584.

[10] T. Nakai, C.A McDowell, Application of Floquet theory to the nuclear magnetic resonance spectra of homonuclear two-spin systems in rotating solids, J. Chem. Phys. 96 (1992) 3452–3466.

[11] S. Dusold, W. Milius, A. Sebald, Iterative lineshape fitting of MAS NMR spectra: a tool to investigate homonuclear J couplings in isolated spin pairs, J. Magn. Reson. 135 (1998) 500–513.

[12] S. Dusold, E. Klaus, A. Sebald, M. Bak, N.C. Nielsen, Magnitudes and relative orientations of chemical shielding, dipolar, and J coupling tensors for isolated ^{31}P–^{31}P spin pairs determined by iterative fitting of ^{31}P MAS NMR spectra, J. Am. Chem. Soc. 119 (1997) 7121–7129.

[13] S. Dusold, H. Maisel, A. Sebald, Magnitudes and orientations of interaction tensors determined from rotational resonance MAS NMR lineshapes of a four-^{13}C spin system, J. Magn. Reson. 141 (1999) 78–90.

[14] M. Bechmann, S. Dusold, A. Sebald, W.A. Shuttleworth, D.L. Jakeman, D.J. Mitchell, J.N.S. Evans, ^{13}C chemical shielding tensor orientations in a phosphoenolpyruvate moiety from ^{13}C rotational-resonance MAS NMR lineshapes, Solid State Sci. 6 (2004) 1097–1105.

[15] M. Bechmann, X. Helluy, A. Sebald, Selectivity of double-quantum filtered rotational-resonance experiments on larger-than-two-spin systems, in: S. Kiihne, H.J.M. de Groot (Eds.), Perspectives on Solid-State NMR in Biology, Kluwer, Dordrecht, The Netherlands, 2001, pp. 23–32.

[16] P.T.F. Williamson, A. Verhoeven, M. Ernst, B.H. Meier, Determination of internuclear distances in uniformly labeled molecules by rotational-resonance in solid-state NMR, J. Am. Chem. Soc. 124 (2003) 2718–2722.

[17] N.C.N. Nielsen, F. Creuzet, R.G. Griffin, M.H. Levitt, Enhanced double-quantum nuclear magnetic resonance in spinning solids at rotational resonance, J. Chem. Phys. 96 (1992) 5668–5677.

[18] T. Karlsson, M. Edén, H. Luthman, M.H. Levitt, Efficient double-quantum excitation in rotational resonance NMR, J. Magn. Reson. 145 (2000) 95–107.

[19] S. Dusold, A. Sebald, Double-quantum filtration under rotational-resonance conditions: numerical simulations and experimental results, J. Magn. Reson. 145 (2000) 340–356.

[20] M. Bechmann, X. Helluy, A. Sebald, Double-quantum filtered rotational-resonance MAS NMR in the presence of large chemical shielding anisotropies, J. Magn. Reson. 152 (2001) 14–25.

[21] M. Bechmann, X. Helluy, C. Marichal, A. Sebald, Double-quantum filtered MAS NMR in the presence of chemical shielding anisotropies and direct dipolar and J couplings, Solid State Nucl. Magn. Reson. 21 (2002) 71–85.

[22] P.R. Costa, B. Sun, R.G. Griffin, Rotational resonance tickling: accurate internuclear distance measurements in solids, J. Am. Chem. Soc. 119 (1997) 10821–10830.

[23] K. Takegoshi, S. Nakamura, T. Terao, ^{13}C–^{1}H dipolar-assisted rotational-resonance in magic-angle spinning NMR, Chem. Phys. Lett. 344 (2001) 631–637.

[24] M.M. Maricq, J.S. Waugh, NMR in rotating solids, J. Chem. Phys. 70 (1979) 3300–3316.

[25] P. Tekely, C. Gardiennet, M.J. Potrzebowski, D. Reichert, Z. Luz, A. Sebald, Probing molecular geometry of solids by NMR spin exchange at the $n = 0$ rotational-resonance condition, J. Chem. Phys. 116 (2002) 7607–7616.

[26] M. Bechmann, S. Dusold, F. Geipel, A. Sebald, D. Sellmann, Magnitudes and orientations of ^{31}P chemical shielding tensors in Pt(II)-phosphine complexes and other four-fold coordinated phosphorus sites, 2004 (submitted).

[27] R.R. Ernst, G. Bodenhausen, A. Wokaun, Principles of Nuclear Magnetic Resonance in One and Two Dimensions, Clarendon Press, Oxford, 1987.

[28] M.H. Levitt, The signs of frequencies and phases in NMR, J. Magn. Reson. 126 (1997) 164–182.

[29] U. Haeberlen, High resolution NMR in solids. Selective averaging, in: J.S. Waugh (Ed.), Advances in Magnetic Resonance, Academic Press, New York, (Suppl. 1), 1976.

[30] A.R. Edmonds, Angular Momentum in Quantum Mechanics, Princeton University Press, Princeton, 1974.

[31] M. Bak, N.C. Nielsen, REPULSION, a novel approach to efficient powder averaging in solid-state NMR, J. Magn. Reson. 125 (1997) 132–139.

[32] S.A. Smith, T.O. Levante, B.H. Meier, R.R. Ernst, Computer simulations in magnetic resonance. An object oriented programming approach, J. Magn. Reson. A 106 (1994) 75–105.

[33] M. Edén, Y.K. Lee, M.H Levitt, Efficient simulation of periodic problems in NMR: application to decoupling and rotational resonance, J. Magn. Reson. A 120 (1996) 56–71.

[34] T. Charpentier, C. Fermon, J. Virlet, Efficient time propagation technique for MAS NMR simulation: application to quadrupolar nuclei, J. Magn. Reson. 132 (1998) 181–190.

[35] M.H. Levitt, M. Edén, Numerical simulation of periodic NMR problems: fast calculation of carousel averages, Mol. Phys. 95 (1998) 879–890.
[36] M. Hohwy, H. Bildsoe, H.J. Jakobsen, N.C. Nielsen, Efficient spectral simulations in NMR of rotating solids. The γ-COMPUTE algorithm, J. Magn. Reson. 136 (1999) 6–14.
[37] F. James, M. Roos, MINUIT computer code, Program D-506, CERN, Geneva, 1977.
[38] MATLAB, Version 6.0; The Mathworks Inc., Natick, MA, 2001.
[39] P. Hodgkinson, L. Emsley, The reliability of the determination of tensor parameters by solid-state nuclear magnetic resonance, J. Chem. Phys. 107 (1997) 4808–4816.
[40] M. Bechmann, K. Hain, C. Marichal, A. Sebald, X-{^{1}H,^{19}F} triple resonance with a X-{^{1}H} CP MAS probe and characterisation of a ^{29}Si–^{19}F spin pair, Solid State Nucl. Magn. Reson. 23 (2003) 50–61.
[41] T. Karlsson, J.M. Popham, J.R. Long, N. Oyler, G.P. Drobny, A study of homonuclear dipolar recoupling sequences in solid-state nuclear magnetic resonance, J. Am. Chem. Soc. 125 (2003) 7394–7407.
[42] M. Carravetta, M. Edén, O.G. Johannessen, H. Luthman, P.E. Verdegem, J. Lugtenburg, A. Sebald, M.H. Levitt, Estimation of carbon–carbon bond lengths and medium-range internuclear distances by solid-state nuclear magnetic resonance, J. Am. Chem. Soc. 123 (2001) 10628–10638.